



**HAL**  
open science

## Using remotely sensed solar radiation data for reference evapotranspiration estimation at a daily time step

Benjamin Bois, Philippe Pieri, Cornelis van Leeuwen, Lucien Wald, Frédéric Huard, Jean-Pierre Gaudillère, Etienne Saur

### ► To cite this version:

Benjamin Bois, Philippe Pieri, Cornelis van Leeuwen, Lucien Wald, Frédéric Huard, et al.. Using remotely sensed solar radiation data for reference evapotranspiration estimation at a daily time step. *Agricultural and Forest Meteorology*, 2007, 148 (4), pp.619-630. 10.1016/j.agrformet.2007.11.005 . hal-00335548

**HAL Id: hal-00335548**

**<https://hal.science/hal-00335548v1>**

Submitted on 29 Nov 2008

**HAL** is a multi-disciplinary open access archive for the deposit and dissemination of scientific research documents, whether they are published or not. The documents may come from teaching and research institutions in France or abroad, or from public or private research centers.

L'archive ouverte pluridisciplinaire **HAL**, est destinée au dépôt et à la diffusion de documents scientifiques de niveau recherche, publiés ou non, émanant des établissements d'enseignement et de recherche français ou étrangers, des laboratoires publics ou privés.

# Using remotely sensed solar radiation data for reference evapotranspiration estimation at a daily time step

B. Bois<sup>a</sup>, P. Pieri<sup>a</sup>, C. Van Leeuwen<sup>b,\*</sup>, L. Wald<sup>c</sup>, F. Huard<sup>d</sup>, J.-P. Gaudillere<sup>a</sup>, E. Saur<sup>b</sup>

<sup>a</sup>UMR Ecophysiologie et Génomique Fonctionnelle de la Vigne, ISVV, Université Bordeaux 2 - INRA, BP 81,  
33883 Villenave d'Ornon Cedex, France

<sup>b</sup>Ecole Nationale d'Ingénieurs des Travaux Agricoles de Bordeaux, 1 cours du Général de Gaulle, 33175  
Gradignan Cedex, France

<sup>c</sup>CEP, Ecole de Mines de Paris, BP 207, F-06904 Sophia Antipolis Cedex, France

<sup>d</sup>UE AgroClim, INRA, Domaine de Saint-Paul, Site Agroparc, 84914 Avignon Cedex 9, France

\*Corresponding author, Tel.: +33 5 57 35 07 55; Fax: +33 5 57 35 07 59. Email: k-van-leeuwen@enitab.fr

## Abstract

Solar radiation is an important climatic variable for assessing reference evapotranspiration ( $E_0$ ), but it is seldom available in weather station records. Meteosat satellite images processed with the Heliosat-2 method provide the HelioClim-1 database, which displays spatialized solar radiation data at a daily time step for Europe and Africa. The aim of the present work was to investigate the interest of satellite-sensed solar radiation for  $E_0$  calculation, where air temperature is the sole local weather data available. There were two study areas in Southern France. One (Southwest, SW) is characterized by oceanic climate and the other (Southeast, SE) by Mediterranean climate. A data set of daily values for 19 weather stations spanning five years (2000–2004) was used. First, a sensitivity analysis of the Penman-Monteith formula to climate input variables was performed, using the Sobol' method. It shows that  $E_0$  is mainly governed by solar radiation during summer, and by wind speed during winter. Uncertainties of HelioClim-1 solar radiation data and their repercussions on  $E_0$  formulae were evaluated, using the FAO-56 Penman-Monteith formulae (*PM*) and radiation-based methods (Turc, *TU*; Priestley-Taylor, *PT* and Hargreaves-Radiation, *HR*). It was shown that HelioClim-1 data slightly underestimate solar radiation and provide relative RMSE (root mean squared error) of 20% of the mean annual value for SW and 14% for SE. The propagation of HelioClim-1 data uncertainties is small in *PM* but considerable in radiation methods. Four estimation methods were then compared to *PM* data: the 1985 Hargreaves formula (*HT*) based on air temperature only; *TU*, *PT* and *HR*, based on air temperature and satellite sensed solar radiation. Radiation methods were more precise and more accurate than *HT*, with RMSE ranging from 0.52 mm to 0.86 mm against 0.67 mm to 0.96 mm. These results suggest that using satellite-sensed solar radiation may improve  $E_0$  estimates for areas where air temperature is the only available record at ground level.

**Keywords:** evapotranspiration, solar radiation, Penman-Monteith equation, sensitivity analysis, remote sensing.

## 1 Introduction

Reference evapotranspiration ( $E_0$ ) is an agrometeorological variable widely used in hydrology and agriculture. Together with precipitation, it is a major input in soil water balance models. Several of these models require daily or hourly evapotranspiration data to provide acceptable estimate of plants water requirements (Brisson et al., 1992 ; Guyot, 1997 ; Lebon et al., 2003). Penman-Monteith combination method is one of the most accurate methods to evaluate  $E_0$  at different time steps. A standardization of this method has been proposed by the Food and Agriculture Organization (Allen *et al.*, 1998). It is known as FAO-

52 56 Penman-Monteith application, and it can be considered as a worldwide standard. However,  
53 it requires numerous weather variables (air temperature, relative humidity, wind speed and  
54 solar radiation), which are seldom available in basic meteorological records. Consequently,  
55 reference evapotranspiration is often estimated by means of empirical equations based on air  
56 temperature, relative humidity, extraterrestrial radiation and/or precipitation (Droogers and  
57 Allen, 2002 ; Hargreaves et al., 1985 ; Popova et al., 2005 ; Turc, 1961). Several authors  
58 proposed modifications of existing empirical methods (Droogers and Allen, 2002 ; Gavilan et  
59 al., 2006 ; Pereira, 2004 ; Pereira and Pruitt, 2004 ; Popova et al., 2005 ; Xu and Singh, 2002).  
60 The accuracy of these methods remains acceptable when applied at large time and space  
61 scales (e.g., a decade and distances larger than 1000 km). However, empirical formulae are  
62 limited by their inherent characteristics. The lack of one, or more, climate variable physically  
63 related to evaporation and transpiration processes inescapably reduces the accuracy of  
64 evapotranspiration estimation. Even if recalibration of empirical factors may improve locally  
65 the precision of these methods, considerable estimation errors will remain as time variations  
66 of missing climate variables are not considered. An example of this statement is the varying  
67 behavior of empirical formulae according to the type of climate considered (Jensen et al.,  
68 1990). Thus, there is little hope that a universal, accurate and robust empirical formula based  
69 on a limited set of weather variables will ever be proposed.

70 Choudhury (1997) proposed a method to assess  $E_0$  by means of satellite data, such as remotely  
71 sensed solar radiation, air temperature (derived from infrared images and weather station  
72 measurements) and vapor pressure deficit. This method provides good evapotranspiration  
73 estimates for low-resolution applications such as worldwide scale and monthly time step. The  
74 accuracy is limited by the high uncertainties provided by satellite sensed vapor pressure  
75 estimations.

76 Several methods have been recently proposed to estimate solar radiation (Struzik, 2001).  
77 Amongst them, the Heliosat-2 method (Rigollier *et al.*, 2004) has been proved to be  
78 reasonably reliable for estimating daily irradiation over Europe and Africa. This method has  
79 been used to elaborate a database, HelioClim-1, available at <http://www.soda-is.org> (Lefèvre  
80 *et al.*, 2007).

81 Solar radiation strongly controls evaporation from the land surface. As small uncertainties in  
82 solar radiation may have considerable effect on the  $E_0$  calculation (Llasat and Snyder, 1998)  
83 and as the variations in space of the radiation cannot be captured by pyranometers, which are  
84 in any case expensive and fragile devices, it can be assumed that remotely sensed solar  
85 irradiation should be useful for  $E_0$  estimation.

86 In this paper, the relevance of remotely sensed solar radiation for computing  $E_0$  at a daily time  
87 step is tested and discussed. First, a sensitivity analysis of the Penman-Monteith method to  
88 input variables for daily reference evapotranspiration calculation is performed. Then satellite-  
89 sensed solar radiation data is compared to ground data and error propagations in several  $E_0$   
90 methods are evaluated. Finally, the accuracy of several  $E_0$  methods based on solar radiation  
91 data are compared to the  $E_0$  Hargreaves temperature method, to evaluate the benefits provided  
92 by the use of satellite-sensed solar radiation, for areas where air temperature is the only  
93 ground-measured available data.

## 94 95 **2 Methods**

### 96 97 *2.1 Study areas*

98 The study was performed in two regions of France (figure 1). One is located in the Southwest  
99 of France (hereafter referred to as SW). It is mostly flat and is characterized by a temperate  
100 climate under the influence of the Atlantic Ocean. Rainfalls range from 800 mm to 1800 mm  
101 per year; the average value for the area is 1000 mm per year. Summer is dry (mean of 60 mm  
per month), and autumn and winter are wet (approximately 100 mm per month). From 1971

102 to 2000, monthly means of temperatures varied from 5 °C in the winter to 20 °C in the  
103 summer. The second area is the Southeast of France (hereafter referred to as SE). It exhibits  
104 marked orography due to the Southern Alps. The climate is Mediterranean, with hot and dry  
105 summers (20 mm to 40 mm of rainfall per month and an average maximum temperature over  
106 30 °C) and mild and wetter winters (40 mm to 100 mm per month with mean temperature  
107 between 0 °C and 5 °C).

## 108 2.2 Data

### 109 2.2.1 Ground station data

110 Data was collected from 19 INRA-Agroclim weather stations. Eight are situated in Southwest  
111 area and 11 are located in Southeast area (table 1 and figure 1). All stations are Cimel<sup>®</sup>  
112 automatic weather stations, equipped with humidity and thermal sensors under a cylinder type  
113 disc shelter (80 mm x 150 mm), cup anemometer and class 2 pyranometer. Minimum and  
114 maximum temperature, minimum and maximum relative humidity, solar irradiation and wind  
115 speed at 2 meters high at a daily time step were used. Average daily temperature is the mean  
116 of minimum and maximum daily temperatures values. The study was performed on a five  
117 year (2000-2004) data set.

### 118 2.2.2 Satellite sensed solar radiation

119 Remotely sensed solar irradiation was collected from the HelioClim-1 database available at  
120 <http://www.soda-is.org>. This database has been obtained by the application of the Heliosat-2  
121 method to Meteosat satellite images. The Heliosat-2 method is based on the principle of the  
122 construction of a *cloud index* for each given pixel of satellite images (Cano *et al.*, 1986 ;  
123 Rigollier *et al.*, 2004). This index is obtained by calculating ground and cloud albedos from  
124 time-series of images acquired in a broadband channel spanning visible and near-infrared  
125 bands. A clear-sky index is then derived from the cloud index. Irradiation is obtained by  
126 multiplying this clear-sky index by the irradiation that should be observed under clear-sky  
127 conditions; the latter is estimated by means of the model of Rigollier *et al.* (2000). The  
128 precision of the method depends mostly on the cloud cover: relative uncertainties are lower  
129 during clear sky days (Rigollier *et al.*, 2004 ; Lefèvre *et al.*, 2007).

130 The HelioClim-1 database provides daily irradiation data for Europe and Africa. It has been  
131 constructed from a data set of reduced spatial resolution, called ISCCP-B2 data, that was  
132 created for the International Satellite Cloud Climatology Project (ISCCP) to better handle and  
133 exploit the wealth of information provided by the Meteosat series of satellites. The B2 data set  
134 is produced from Meteosat images by firstly performing a time sampling that reduces the  
135 frequency of observation to the standard meteorological synoptic 3-h intervals, starting at  
136 0000 UTC. Secondly, the higher-resolution data in the visible channel are averaged to match  
137 the lower resolution of infrared channel data (i.e. an image of 2500 x 2500 pixels with a  
138 resolution of 5 km). Finally, a spatial sampling is performed by taking 1 pixel over 6 in each  
139 direction (i.e. 1 pixel each 30 km), starting with the south-easternmost pixel. For each  
140 remaining pixel, the irradiation was calculated every 3 h and integrated to provide daily  
141 irradiation. The HelioClim-1 database contains daily irradiation for these pixels (Lefevre et  
142 al., 2007). The irradiation data for any location are obtained by interpolating the daily values  
143 available at the nine closest pixels using inverse distance squared method (Lefèvre *et al.*,  
144 2002). Daily irradiation data were collected for the location of the 19 weather stations for the  
145 period 2000-2004.

## 146 2.3 Reference evapotranspiration methods

### 147 2.3.1 The FAO Penman-Monteith method

151 The Penman-Monteith method combines energy balance and mass transfer concepts (Penman,  
 152 1948) with stomatal and surface resistance (Monteith, 1981).  
 153 Recently, the FAO proposed a standard parameterization of the Penman-Monteith method for  
 154 estimating the evaporation from a well-irrigated, homogenous, 0.12 m grass cover considered  
 155 as a “reference crop” (Allen *et al.*, 1998). This method, hereafter referred as *PM*, is now used  
 156 worldwide and the international agronomy community considers it as a standard. The FAO  
 157 Penman-Monteith reference evapotranspiration (mm) is calculated as follows:

$$158 \quad E_{PM} = \frac{0.408\Delta(R_n) + \gamma \frac{900}{(T + 273)} u_2 (e_s - e_a)}{\Delta + \gamma(1 + 0.34u_2)} \quad (1)$$

159 where  $\Delta$  is the slope of the saturation vapor pressure curve at air temperature [kPa °C<sup>-1</sup>],  $\gamma$  is  
 160 the psychrometric constant [kPa °C<sup>-1</sup>],  $T$  is the average air temperature [°C],  $u_2$  is the wind  
 161 speed measured at 2 m above ground surface [m s<sup>-1</sup>],  $e_s$  and  $e_a$  are the saturation and the actual  
 162 vapor pressure [kPa], respectively, and  $R_n$  is the net radiation [MJ m<sup>-2</sup>], calculated as follows :

$$163 \quad R_n = R_{ns} - R_{nl} \quad (2)$$

164 where  $R_{ns}$  is the net shortwave radiation [MJ m<sup>-2</sup>] given by :

$$165 \quad R_{ns} = (1 - a)R_s \quad (3)$$

166 and  $R_{nl}$  is the net longwave radiation [MJ m<sup>-2</sup>] given by :

$$167 \quad R_{nl} = \sigma \left[ \frac{T_{\max,K}^4 + T_{\min,K}^4}{2} \right] \left( 0.34 - 0.14\sqrt{e_a} \right) \left( 1.35 \frac{R_s}{R_{so}} - 0.35 \right) \quad (4)$$

168 where  $R_s$  is the global solar radiation [MJ m<sup>-2</sup>],  $a$  is the albedo of the hypothetical grass  
 169 reference crop, set to 0.23,  $T_{\max,K}$  and  $T_{\min,K}$  are the maximum and minimum air temperature  
 170 [K], respectively, and  $R_{so}$  is the clear-sky solar radiation [MJ m<sup>-2</sup>], given by :

$$171 \quad R_{so} = (0.75 + 2z10^{-5})R_a \quad (5)$$

172 where  $z$  is the station elevation above sea level [m] and  $R_a$  is the extraterrestrial radiation  
 173 [MJ m<sup>-2</sup>]. Undefined components used in equations (2), (3), (4) and (5) have the same  
 174 signification and units as in equation (1).

175 The actual vapor pressure [kPa], used in equations (1) and (4) is calculated as follows:

$$176 \quad e_a = \frac{e^{\circ}(T_{\min}) \frac{RH_{\max}}{100} + e^{\circ}(T_{\max}) \frac{RH_{\min}}{100}}{2} \quad (6)$$

177 where  $e^{\circ}(T_{\min})$  and  $e^{\circ}(T_{\max})$  are the saturation vapor pressure at minimum and maximum air  
 178 temperature [kPa], respectively,  $RH_{\min}$  is the minimum relative humidity and  $RH_{\max}$  is the  
 179 maximum relative humidity.

180 The slope of saturation vapor pressure curve at air temperature is given by :

$$181 \quad \Delta = \frac{4098[e^{\circ}(T)]}{(T + 237.2)^2} \quad (7)$$

182 where  $e^{\circ}(T)$  is the saturation vapor pressure at average air temperature and  $T$  as the same  
 183 signification and units as in equation (1).

184 *PM* or other Penman-Monteith versions have been proved to be among the most precise and  
 185 accurate models for daily reference evapotranspiration prediction under different climatic  
 186 conditions when compared to lysimetric measurements (Allen *et al.*, 1989 ; Hargreaves and  
 187 Allen, 2003 ; Garcia *et al.*, 2004 ; Pereira, 2004; Pereira and Pruitt, 2004).

188 In this paper,  $E_{PM}$  is considered as the reference value against which other empirical methods  
 189 will be compared. This choice is motivated by the fact that most of the applications based  
 190 upon reference evapotranspiration, such as irrigation schemes, hydrological studies or water  
 191 balance modelling, use calculated  $E_0$  rather than lysimetric measurements.

192

### 193 2.3.2 Empirical methods

194 In this study, radiation methods, *i.e.* empirical methods that calculate  $E_0$  with air temperature  
195 and solar radiation, are singled out, in order to test the relevance of using remotely sensed  
196 solar radiation for  $E_0$  estimates.

197 Three radiation methods and one temperature method were compared to *PM*.

198 Hargreaves radiation method (hereafter referred as to *HR*, Hargreaves and Samani, 1982) was  
199 established in 1975 from a regression with lysimeter data collected at Davis (California, USA)  
200 and the product of temperature and solar radiation, for a five day time step. The following  
201 prediction equation was then proposed:

$$202 \quad E_{HR} = 0.0135 \frac{R_s}{\lambda} (T + 17.8) \quad (8)$$

203 where  $\lambda$  is the latent heat of vaporization = 2.45 MJ kg<sup>-1</sup> at 20 °C (as  $\lambda$  is very stable, this  
204 value was used in the current study), and other components having the same signification and  
205 units as in equations (1) and (3). Hargreaves radiation method has seldom been tested, despite  
206 encouraging results (Hargreaves and Allen, 2003). As solar radiation has rarely been  
207 available, Hargreaves proposed a modified version of this method, so that reference  
208 evapotranspiration could be estimated with minimum and maximum air temperature only  
209 (Hargreaves *et al.*, 1985). This method is known as the 1985 Hargreaves temperature method  
210 (hereafter referred to as *HT*):

$$211 \quad E_{HT} = 0.0023 \frac{R_a}{\lambda} (T + 17.8) \sqrt{(T_{\max} - T_{\min})} \quad (9)$$

212 where  $T_{\min}$  and  $T_{\max}$  are the minimum and the maximum air temperature, respectively [°C].  
213 and undefined components having the same signification and units as in equations (1), (5) and  
214 (8). Local calibrations of the empirical coefficient (0.0023), based upon regional wind speed  
215 and air temperature, were recently proposed (Gavilan *et al.*, 2006).

216

217 The Turc radiation method (hereafter referred to as *TU*; Turc, 1961), initially developed for  
218 10-day periods, provides good results for a humid environment (Jensen *et al.*, 1990).

219 Reference evapotranspiration is calculated as follows:

$$220 \quad E_{TU} = 0.013 (23.88 R_s + 50) \left( \frac{T}{T + 15} \right) \quad (10)$$

221 where  $R_s$  and  $T$  have the same signification and units as in equations (1) and (3).

222 The Priestley-Taylor method (hereafter referred as *PT*, Priestley and Taylor, 1972), unlike  
223 radiation methods presented above, is mostly based on physical principles. The *PT* method is  
224 derived from energy balance concepts and the hypothesis that (at least for short vegetation)  
225 fluxes over land are mostly governed by radiative rather than advected energy. Thus,  $E_0$  is  
226 given by:

$$227 \quad E_{PT} = \alpha \frac{\Delta}{\Delta + \gamma} R_n \quad (11)$$

228 where  $\alpha$  is an empirical and unitless coefficient, set to 1.26, and  $R_n$ ,  $\Delta$  and  $\gamma$  have the same  
229 signification and units as in equation (1). To avoid the use of minimum and maximum relative  
230 humidity for  $E_{PT}$  calculation ( $E_{PT}$  is calculated with air temperature and solar radiation only),  
231 the actual vapour pressure  $e_a$ , required for  $R_n$  calculation (equation (4)) is estimated from  
232 minimum air temperature only:

$$233 \quad e_a = e^\circ(T_{\min}) = 0.611 \exp \left[ \frac{17.27 T_{\min}}{T_{\min} + 237.3} \right] \quad (12)$$

234 where  $e_a$  and  $T_{\min}$  have the same significance and units as in equations (6) and (9).

235 Equation (12) follows the recommendations in Allen *et al.* (1998) to compute  $e_a$  when relative  
 236 humidity is missing.  
 237 *PT* method has been used and tested in many studies, and has shown to be reliable in humid  
 238 climate conditions for evaporation (Xu and Singh, 2000) and reference evapotranspiration  
 239 (Jensen *et al.*, 1990) estimations. Local adjustments of  $\alpha$  are necessary in numerous cases (Xu  
 240 and Singh, 2002; Bois *et al.*, 2005; Fisher *et al.*, 2005), and a calculation method for  $\alpha$  based  
 241 on surface and aerodynamic resistance parameters was proposed by Pereira (2004). A  
 242 recalibration of  $\alpha$  to increase the precision of *PT* estimates, is discussed in the results section,  
 243 but the results presented in this paper focus on the *PT* method with  $\alpha$  set to 1.26, as  
 244 recalibration of empirical formulae is not the main objective of the present study.  
 245

## 246 2.4 Sensitivity analysis

### 247 2.4.1 The Sobol' method

248 To estimate the relative participation of climate variables to *PM* model output, a sensitivity  
 249 analysis was performed. There are several approaches available for sensitivity analysis studies  
 250 (see Frey and Patil, 2002 or Saltelli *et al.*, 2006 for reviews). For the present work, the Sobol'  
 251 based variance method was used (Sobol', 1993). This method allows evaluating the sensitivity  
 252 of a model to interaction between input variables. It consists of numerous simulations of the  
 253 models using two independent samples of  $N$  repetitions (rows) and  $k$  input variables  
 254 (columns), retrieved from existing data or randomly generated data from the probability  
 255 distribution function of each  $k$  input variable. One or several variables in the first sample are  
 256 substituted by the same variable(s) taken from the second sample. For each of the  $(2^k-1)$   
 257 possible combinations of variable substitutions between the two samples,  $N$  runs of the model  
 258 are computed. The sensitivity of the model to input variables is based on so-called sensitivity  
 259 or Sobol' indices, which are calculated on the principle of the decomposition of the total  
 260 variance  $V$  of the model output, in response to individual or simultaneous variations of the  $k$   
 261 model inputs:

$$262 \quad V = \sum_i V_i + \sum_{i<j} V_{ij} + \sum_{i<j<m} V_{ijm} + \dots + V_{1,2,\dots,k} \quad (13)$$

263 Where  $V_i$  is the model output variance in response to variation of the  $i$ th input variable,  $V_{ij}$  is  
 264 the model output variance in response to the simultaneous variation of the  $i$ th and the  $j$ th  
 265 model input, and so-on. Then, sensitivity indices are calculated as follows:

$$266 \quad S_i = \frac{V_i}{V} \quad (14)$$

$$267 \quad S_{Ti} = \frac{V_i + \sum_j V_{ij} + \sum_{j<m} V_{ijm} + \dots + V_{i,j,\dots,k}}{V} \quad (15)$$

268 where  $j$  and  $m$  are the  $j$ th and the  $m$ th model input variables, and  $i \neq j \neq m$ .  $S_i$  is called the first  
 269 order sensitivity index. It measures the sensitivity of the model to the input variable  $X_i$ .  $S_{Ti}$  is  
 270 called the total sensitivity index. It measures the impact of variations of the  $i$ th model input on  
 271 the model output, including all the possible interactions with other input variations. For more  
 272 details about the Sobol' method, see Saltelli (2002).  
 273

### 274 2.4.2 Sensitivity analysis of *PM* reference evapotranspiration formula

275 A major constraint, when trying to perform a sensitivity analysis, is the interdependency of  
 276 input variables. Considering the Penman-Monteith FAO-56 formula, required input data are  
 277 minimum and maximum air temperature, minimum and maximum relative humidity, solar  
 278 radiation and wind speed. Minimum and maximum air temperature and relative humidity, if  
 279 picked randomly in a data set, will lead to nonsense computations, i.e. having a minimum air

280 temperature or relative humidity value higher than the maximum. To solve this problem  
 281 average air temperature and relative humidity and their daily amplitudes were calculated prior  
 282 to elaborating the two random data sets required for Sobol' method:

$$283 \quad T = \frac{T_{\min} + T_{\max}}{2} \quad ; \quad RH = \frac{RH_{\min} + RH_{\max}}{2} \quad (16) ; (17)$$

284 and

$$285 \quad \Delta T = T_{\max} - T_{\min} \quad ; \quad \Delta RH = RH_{\max} - RH_{\min} \quad (18) ; (19)$$

286 where  $T$  and  $RH$  are the daily average air temperature [°C] and the daily average relative  
 287 humidity [%],  $\Delta T$  [°C] and  $\Delta RH$  [%] are their daily amplitude, and  $T_{\min}$ ,  $T_{\max}$ ,  $RH_{\min}$  and  
 288  $RH_{\max}$  having the signification and units as in equations (6) and (9). Once random samples are  
 289 created,  $T$ ,  $RH$ ,  $\Delta T$  and  $\Delta RH$  are used to retrieve minimum and maximum air temperature and  
 290 relative humidity daily values, inverting the equations (16), (17), (18) and (19).

291 A major requirement of sensitivity analysis is the choice of the input data set. The aim of the  
 292 present SA is to retrieve the climate variables which  $PM$  model is most sensitive to, according  
 293 to different climatic conditions, i.e. Oceanic and Mediterranean climates. It is assumed that  
 294 the climate stations within both study areas (8 for SW and 11 for SE) provide a good sample  
 295 of the spatial variation of climatic conditions. To take into account the variability of climate  
 296 during the year, sensitivity analyses were performed for each month. That is, the input data set  
 297 for Sobol' SA is generated for a given month, according to the probability distribution  
 298 function (PDF) of each input data, recorded at the stations of a given study area (SW or SE).  
 299 For each month and each area, Sobol' SA was assessed as follows (figure 2): (a) empirical  
 300 PDF of each input variable were fitted to empirical distributions of the data sets recorded at  
 301 the (8 or 11) climate stations area during 2000 to 2004, using a Gaussian Kernel fitting  
 302 function with R statistical software (R Development Core Team, 2007) ; (b) Two samples  
 303 were generated by quasi-random sampling with 10000 repetitions ; (c) Several model outputs  
 304 and variance decomposition were computed using Sobol' algorithm of the package *sensitivity*  
 305 of R statistical software ; (d) First order and total sensitivity indexes and their monthly  
 306 evolution were then compared. Note that for step (b), one could propose the use of the  
 307 original data record rather than random sample generations. However, the number of available  
 308 data for each month was not sufficient for the statistical robustness of the analysis.

### 310 2.5 Statistical indices used for satellite sensed solar radiation and empirical $E_0$ formulae 311 evaluations

312 The reference data used to evaluate satellite-sensed solar radiation were pyranometer records  
 313 at ground level. For evapotranspiration,  $PM$  (equation (1)), using pyranometer records, was  
 314 used as a reference data for empirical formulae evaluation. For each day  $i$ , the difference  
 315 between reference and estimated data was calculated as follows :

$$316 \quad D_i = Est_i - Ref_i \quad (20)$$

317 where  $D$  is the difference (or "error") [mm],  $Est_i$  is the satellite-sensed solar radiation or the  
 318  $E_0$  estimated with an empirical method and  $Ref_i$  is the reference data. The units are MJ m<sup>-2</sup> or  
 319 mm according to the type of data evaluated.

320 The accuracy of each method is given by the bias (or mean error):

$$321 \quad bias = \frac{1}{n} \sum_{i=1}^n D_i \quad (21)$$

322 The unit of  $bias$  is mm or MJ m<sup>-2</sup>, according to the type of data evaluated, and  $n$  is the number  
 323 of days.

324 The precision is given by the root mean squared error (RMSE):



325

$$RMSE = \sqrt{\frac{1}{n} \sum_{i=1}^n D_i^2} \quad (25)$$

326

Errors populations were also analyzed by means of coefficient of determination ( $R^2$ ).

327

### 328 **3 Results and discussion**

#### 329 *3.1 Sensitivity analysis of PM formula*

330 *Sensitivity of  $E_0$  computation using PM method in Southwest area (Oceanic climate).* The  
331 results of monthly sensitivity analyses computed using Southwest area data show clear  
332 seasonal trends (figure 3A). During the winter period (from November to February), wind  
333 speed is the main source of variation in  $E_0$  values calculated using *PM* method (e.g. 38% of  $E_0$   
334 total variance in January, table 2). Then come relative humidity and air temperature (32% and  
335 17% of  $E_0$  total variance in January, respectively). Solar radiation, daily amplitude of air  
336 temperature and daily amplitude of relative humidity have little impact on evapotranspiration  
337 process during winter. This trend changes during March and October. From April to  
338 September,  $E_0$  is mostly sensitive to solar radiation (up to 74% of  $E_0$  total variance in May,  
339 and 70% in July). From May to July, *PM* formula is not very sensitive to *RH*,  $U_2$ ,  $\Delta RH$  and  
340  $\Delta T$ . Mean daily air temperature participate from 11% to 15% of  $E_0$  variance, from May to  
341 September. Total sensitivity indices show that, when added to other variables variations, air  
342 temperature has a greater impact on  $E_0$  variability during summer, and wind speed has a  
343 greater impact during winter (figure 3B).

344 *Sensitivity of  $E_0$  computation using PM method in Southeast area (Mediterranean climate).*

345 The sensitivity of *PM* formula to climate input variables in Mediterranean climate conditions  
346 is very close to the one observed for Oceanic climate. Wind speed as a major impact on  $E_0$   
347 calculation during winter and solar radiation is clearly the most influent variable during  
348 summer (figures 3C and 3D, table 2).

349 The present analysis highlights the great sensitivity of this Penman-Monteith formula to solar  
350 radiation during summer period, when  $E_0$  reaches its highest values, and when its calculation  
351 is critical for irrigation process and ecological modelling. These results were obtained for  
352 Mediterranean and Oceanic climate, at medium latitudes. They are consistent with former  
353 uncertainty and sensitivity analyses performed in Mediterranean climate (Llasat and Snyder,  
354 1998 ; Rana and Katerji, 1998). A recent work published by Gong et al. (2006) on a large  
355 range of climatic conditions in Southern China leads to similar results, except for relative  
356 humidity which had a greater impact on  $E_0$  during winter than it has been shown in the  
357 present study.

358 Considering the results of Penman-Monteith sensitivity to solar radiation, it seems reasonable  
359 to evaluate the benefits of satellite sensed solar radiation to  $E_0$  calculation when no solar  
360 radiation ground records are available. This point is studied and discussed in the next section.

361

#### 362 *3.2 Remotely sensed solar radiation performances*

363 Table 3 shows the annual error statistics of solar radiation and  $E_0$  data calculated with  
364 HelioClim-1 data instead of pyranometer radiation data. HelioClim-1 underestimates daily  
365 irradiation (figures 4A and 4D). The bias is twice as important for Southwest area (-  
366 1.87 MJ m<sup>-2</sup>) as it is for Southeast area (-1.07 MJ m<sup>-2</sup>). RMSE is also higher for SW (20% of  
367 the annual solar irradiation) than for SE (14%). Although the uncertainty, in absolute value, is  
368 larger during summer period (Figure 5A), the RMSE are 15% (SW) and 10% (SE) of  $R_S$   
369 pyranometer value in July, whereas they reach 26% (SW) and 18% (SE) in January, as  
370 irradiation is larger during summer.

371 These errors are consistent with those observed in Northern Europe, during former  
372 evaluations of HelioClim-1 database (Lefèvre *et al.*, 2007). When no pyranometer data is

373 available, daily satellite sensed solar radiation should be preferred to temperature-based  
374 estimations: for both areas, daily irradiation RMSE are 3 to 4 times smaller than those  
375 obtained by Hunt *et al.* (2000) in Ontario (Canada), with empirical formulae based on air  
376 temperature. Moreover, HelioClim-1 irradiation may be as precise as pyranometer  
377 measurements where weather stations are not steadily maintained or not equipped with  
378 accurate devices: uncertainty reported varies from 5 to 25%, according to the class of material  
379 and the metrology experts (Llasat and Snyder, 1998 ; Droogers and Allen, 2002).  
380 There are several sources of uncertainties when comparing satellite data to very local  
381 measurements, such as weather station records. This point has been widely discussed by  
382 Zelenka *et al.* (1999). First, it is difficult to compare pixel data, corresponding to a surface,  
383 with a discrete measurement, such as pyranometer weather station records. Another category  
384 of uncertainties comes from the spatial (1 pixel each 30 kilometer) and temporal (3 hours)  
385 resolutions of the initial data set used to create the HelioClim-1 database. In addition, the  
386 spatial interpolation method generates its intrinsic uncertainties. The Heliosat-2 method itself,  
387 used to elaborate the HelioClim-1 database, also participate to uncertainties of satellite sensed  
388 irradiation data (e.g. the algorithm limits). The uncertainties inherent to the ISCCP-B2 data  
389 set could be avoided by applying the Heliosat-2 method to each original Meteosat pixel and  
390 for every hour. The HelioClim-2 database was created in that respect but begins only in 2004  
391 and could not be used in this study.

392

### 393 3.3 Propagation of satellite sensed solar radiation errors in $E_0$ formulae

394 Replacing pyranometer measurement by Heliosat-2 estimations (*i.e.* HelioClim-1 data)  
395 induces little error for reference evapotranspiration calculation using the Penman-Monteith  
396 model (table 3). Estimation errors are higher for middle range  $E_0$  values (figure 4B and 4E).  
397 This could be explained by the fact that most of the errors occur for partially cloudy days, due  
398 to uncertainties in retrieving daily solar radiation with Heliosat-2 method for this type of  
399 weather (Rigollier *et al.*, 2004). In both areas,  $E_{PM}$  is slightly underestimated. For SW, biases  
400 vary from -0.34 mm to 0.01 mm, according to the season (figure 5B). The annual RMSE  
401 value remains low (11% of  $E_0$  mean value). In SE area,  $E_{PM}$  bias is negligible (-0.20 mm to  
402 0.01 mm, figure 5C). Relative RMSE in SE is 7% of  $E_0$  mean value, which is lower than in  
403 SW. Heliosat-2 method is more successful for clear sky days, which could explain the  
404 difference between the two regions, as clear sky situations occur more frequently in SE than  
405 SW. Relative errors of  $E_{PM}$  calculated with HelioClim-1 are lower during summer (9% for  
406 SW and 5% for SE, in July). Again, the better performance of Heliosat-2 method for clear sky  
407 days could explain this seasonal trend, as clear sky situations are more numerous during  
408 summer than during the other seasons. Yet, higher relative errors could have been expected:  
409 sensitivity analyses have shown that solar radiation has the greatest impact on  $PM$  model  
410 during summer (*i.e.* when evapotranspiration reaches its maximum) in Oceanic or  
411 Mediterranean climates (see section 3.1).

412 Errors are higher when pyranometer data is replaced by HelioClim-1 data in radiation  
413 methods, *i.e.*  $HR$ ,  $TU$  and  $PT$  (figure 4C and 4F, table 3). Biases are mostly negative.  
414 Sensitivity to solar radiation errors is higher for radiation methods than for  $PM$  because  
415 radiation methods do not include advective effects on the evapotranspiration process and thus  
416 are mainly governed by radiative transfers. The largest error propagation can be observed for  
417 the Hargreaves radiation method (table 3, figures 5B and 5C).

418

### 419 3.4 Empirical formulae performance

420 Daily  $E_0$  values of 4 empirical methods were compared to reference evapotranspiration  
421 computed with  $PM$ . HelioClim-1 solar radiation was used for radiation methods, whereas

422 pyranometer data was used for *PM*, as it was considered here as the “control” method. Data  
423 sources used for  $E_0$  calculations are shown in table 4.  
424 In both areas, Hargreaves temperature method (*HT*) gave the highest uncertainties for the  
425 annual period (table 5). During summer, formulae using satellite-sensed solar radiation  
426 improve considerably  $E_0$  estimation compared to *HT* estimates based solely on local air  
427 temperature. Figures 6A and 6B show an obvious seasonal trend of *HT* errors, which is  
428 related to the variations in sensitivity of  $E_0$  to the different input variables of *PM*: during  
429 summer, when  $E_0$  is mainly governed by solar radiation, estimates based upon air temperature  
430 only are thus less accurate.  
431 Evapotranspiration calculated with satellite-sensed solar radiation is mainly underestimated.  
432 For both climates, all radiation methods show biases similar to those induced by replacement  
433 of pyranometer data by satellite-sensed solar radiation (between -0.4 mm and -0.2 mm, table 3  
434 and 5): this suggests that the underestimation observed is mainly due to the propagation of  
435 HelioClim-1 data bias within radiation methods, rather than wrong calibration of empirical  
436 coefficients used in these formulae.  
437 In the Southwest area, *PT* data is strongly correlated to *PM* data ( $R^2 = 0.938$ , table 5). It is  
438 also the formula providing the lowest  $E_0$  RMSE during summer and for the whole year (figure  
439 6A). Turc and Hargreaves radiation method performances are almost the same. The  
440 performance of *TU* is slightly better than other formulae from September to November. It has  
441 been shown in former studies that the Turc method provides good results in humid  
442 environment (Jensen et al., 1990 ; Turc, 1961), whereas Hargreaves radiation method has  
443 been established from arid or semi-arid climate data analysis (Hargreaves and Allen, 2003).  
444 These differences between those two formulae did not emerge from the current study, in  
445 Southwest oceanic climate. Hargreaves temperature method provided the lowest RMSE and  
446 the lowest bias (in absolute value), from January to April. However, this temperature-based  
447 method was the least accurate method for SW, when considering summer and annual periods  
448 (RMSE = 0.67 mm,  $R^2=0.894$ , for the whole year). *HT* overestimated  $E_0$  (a mean error of  
449 0.32 mm).  
450 For the Southeast area, all empirical formulae showed poorer performances when compared to  
451 the Southwest region (figure 6B). The higher wind speed and the lower relative humidity in  
452 SW throughout the year might explain these differences (results not shown). *HR* provided the  
453 most precise  $E_0$  estimates for the whole year (RMSE= 0.77 mm, i.e. 25% of  $E_0$  mean annual  
454 value). The best correlation with *PM* values is provided by *PT*. The Priestley-Taylor formula  
455 performed better than every other formula during summer, but showed considerable bias and  
456 RMSE during winter. The lowest bias (in absolute value) is provided by *HT*, which showed in  
457 contrast high RMSE (0.96 mm, i.e. 31% of the annual mean).  
458 These results suggest that using satellite sensed-solar radiation within empirical formulae  
459 improve the accuracy of  $E_0$  estimates during summer and for the whole year, although  
460 reference evapotranspiration remains underestimated in most cases.

#### 462 **4 Conclusions**

463 The present work focused on the role of solar radiation data in reference evapotranspiration  
464 calculation at daily time steps. A sensitivity analysis of the Penman-Monteith model showed  
465 that solar radiation strongly governs reference evapotranspiration during summer, for Oceanic  
466 and Mediterranean climates at medium latitude. The use of satellite-sensed solar radiation  
467 taken from HelioClim-1 database for  $E_0$  calculation was evaluated. It was shown that  
468 HelioClim-1 data underestimates solar radiation at daily time step, for Oceanic and  
469 Mediterranean climates in France. The RMSE ranges from 14 to 20% of the annual solar  
470 radiation. The error propagation is considerable in radiation-based methods, as these  
471 equations are linearly linked to solar radiation input.

472 Amongst the numerous studies concerning reference evapotranspiration estimates with  
473 limited climatic data, few considered daily time step. When temperature data is the sole  
474 climate variable available, Hargreaves temperature method is often used or recommended and  
475 provides relative RMSE ranging from 20% to 30% of the mean annual value, depending on  
476 the type of climate (Droogers and Allen, 2002 ; Hargreaves and Allen, 2003). In the present  
477 work, we found that using satellite sensed global radiation via *PT* or *HR* methods improves  $E_0$   
478 estimates, compared to Hargreaves temperature method. With these empirical solar radiation-  
479 based methods, relative annual RMSE ranges from 22% to 28 %, according to the method and  
480 the type of climate, humid-Oceanic or semi-arid-Mediterranean. Hargreaves temperature  
481 method, however, produced annual RMSE of 28% of the annual mean for Oceanic climate  
482 and 31% for Mediterranean climate. The difference in precision between radiation and  
483 Hargreaves temperature method reaches its maximum during summer, when the  $E_0$  process is  
484 mainly governed by solar radiation. In contrast, *HT* showed smaller uncertainties than  
485 radiation methods with HelioClim-1 data during winter.  
486 These results suggest that during summer, using empirical radiation methods with satellite  
487 sensed solar radiation from the HelioClim-1 database to estimate  $E_0$  should be preferred to  
488 *HT*, when air temperature is the only available record at weather stations.  
489 These observations need to be verified in other climatic conditions, and especially in arid  
490 climates, where  $E_0$  estimation is crucial for water management. This could be easily done  
491 using HelioClim-1 database, as it provides data for a large surface of the globe, i.e. from  
492 Northern Europe to South-Africa.

493

#### 494 **Acknowledgements**

495 The authors would like to thank the Conseil Interprofessionnel des Vins de Bordeaux for their  
496 financial and technical support. Thanks to the Center for Energy and Processes (Centre  
497 Energétique et Procédés, Sophia-Antipolis, France) for providing HelioClim-1 data.

498 **References**

- 499 Allen, R.G., Jensen, M.E., Wright, J.L. and Burman, R.D., 1989. Operational estimates of  
500 reference evapotranspiration. *Agronomy Journal*, 81(4): 650-662.
- 501 Allen, R.G., Pereira, L.S., Raes, D. and Smith, M., 1998. Crop evapotranspiration: guidelines  
502 for computing crop water requirements. FAO Irrigation and Drainage Paper. Food and  
503 Agriculture Organization (FAO), Rome Italy, 300 pp.
- 504 Bois, B., Pieri, P., Van Leeuwen, C. and Gaudillere, J.P., 2005. Sensitivity analysis of the  
505 Penman-Monteith evapotranspiration formula and comparison of empirical methods  
506 used in viticulture soil water balance, XIV International GESCO Viticulture Congress,  
507 Geisenheim, Germany, 23-27 August, 2005.
- 508 Brisson, N., Seguin, B. and Bertuzzi, P., 1992. Agrometeorological soil water balance for  
509 crop simulation models. *Agricultural and Forest Meteorology*, 59(3-4): 267-287.
- 510 Cano, D., Monget, J.-M., Albuissou, M., Guillard, H., Regas, N. and Wald L., 1986. A  
511 method for the determination of the global solar radiation from meteorological  
512 satellites data. *Solar Energy*, 37(1): 31-39.
- 513 Cukier, R.I., Levine, H.B. and Shuler, K.E., 1978. Nonlinear sensitivity analysis of  
514 multiparameter model systems. *Journal of Computational Physics*, 26(1): 1-42.
- 515 Choudhury, B.J., 1997. Global pattern of potential evaporation calculated from the Penman-  
516 Monteith equation using satellite and assimilated data. *Remote Sensing of*  
517 *Environment*, 61(1): 64-81.
- 518 Droogers, P. and Allen, R.G., 2002. Estimating reference evapotranspiration under inaccurate  
519 data conditions. *Irrigation and Drainage Systems*, 16(1): 33-45.
- 520 Fisher, J.B., DeBiase, T.A., Qi, Y., Xu, M. and Goldstein, A.H., 2005. Evapotranspiration  
521 models compared on a Sierra Nevada forest ecosystem. *Environmental Modelling &*  
522 *Software*, 20(6): 783-796.
- 523 Frey, H.C. and Patil, S.R., 2002. Identification and review of sensitivity analysis methods.  
524 *Risk Analysis*, 22(3): 553-578.
- 525 Garcia, M., Raes, D., Allen, R. and Herbas, C., 2004. Dynamics of reference  
526 evapotranspiration in the Bolivian highlands (Altiplano). *Agricultural and Forest*  
527 *Meteorology*, 125(1/2): 67-82.
- 528 Gavilan, P., Lorite, I.J., Tornero, S. and Berengena, J., 2006. Regional calibration of  
529 Hargreaves equation for estimating reference ET in a semiarid environment.  
530 *Agricultural Water Management*, 81(3): 257-281.
- 531 Gong, L., Xu, C.-y., Chen, D., Halldin, S. and Chen, Y.D., 2006. Sensitivity of the Penman-  
532 Monteith reference evapotranspiration to key climatic variables in the Changjiang  
533 (Yangtze River) basin. *Journal of Hydrology*, 329(3/4): 620-629.
- 534 Guyot, G., 1997. *Climatologie de l'environnement. De la plante aux écosystèmes*. Masson,  
535 Paris, 505 pp.
- 536 Hargreaves, G.H. and Allen, R.G., 2003. History and Evaluation of Hargreaves  
537 Evapotranspiration Equation. *Journal of Irrigation and Drainage Engineering*, 129(1):  
538 53-63.
- 539 Hargreaves, G.H. and Samani, Z.A., 1982. Estimating Potential Evapotranspiration. *Journal*  
540 *of the Irrigation and Drainage Division*, 108: 223-230.
- 541 Hargreaves, G.L., Hargreaves, G.H. and Riley, J.P., 1985. Agricultural benefits for Senegal  
542 River Basin. *Journal of Irrigation and Drainage Engineering*, 111: 111-124.
- 543 Hunt, L. A., Kuchar, L. and Swanton, C. J., 1998. Estimation of solar radiation for use in crop  
544 modelling. *Agricultural and Forest Meteorology* 91 (3/4): 293-300.
- 545 Jensen, M.E., Burman, R.D. and Allen, R.G., 1990. Evapotranspiration and Irrigation Water  
546 Requirements. *ASCE Manuals and Reports on Engineering Practices*, 70. American  
547 Society of Civil Engineers, New York, 360 pp.

548 Lebon, E., Dumas, V., Pieri, P. and Schultz, H.R., 2003. Modelling the seasonal dynamics of  
549 the soil water balance of vineyards. *Functional Plant Biology*, 30(6): 699-710.

550 Lefèvre, M., Remund, J., Albuissou, M. and Wald, L., 2002. Study of effective distances for  
551 interpolation schemes in meteorology. *Geophysical Research Abstracts*, 4, April 2002,  
552 EGS02-A-03429, European Geophysical Society.

553 Lefevre, M., Wald, L. and Diabate, L., 2007. Using reduced data sets ISCCP-B2 from the  
554 Meteosat satellites to assess surface solar irradiance. *Solar Energy*, 81(2): 240-253.

555 Llasat, M.C. and Snyder, R.L., 1998. Data error effects on net radiation and  
556 evapotranspiration estimation. *Agricultural and Forest Meteorology*, 91(3/4): 209-221.

557 Monteith, J.L., 1981. Evaporation and surface temperature. *Quarterly Journal Of The Royal*  
558 *Meteorological Society*, 107(451): 1-27.

559 Penman, H.L., 1948. Natural evaporation from open water, bare soil and grass. *Proceedings of*  
560 *the Royal Society of London*, A193: 120-146.

561 Pereira, A.R., 2004. The Priestley-Taylor parameter and the decoupling factor for estimating  
562 reference evapotranspiration. *Agricultural and Forest Meteorology*, 125(3/4): 305-313.

563 Pereira, A.R. and Pruitt, W.O., 2004. Adaptation of the Thornthwaite scheme for estimating  
564 daily reference evapotranspiration. *Agricultural Water Management*, 66(3): 251-257.

565 Popova, Z., Kercheva, M. and Pereira, L.S., 2005. Validation of the FAO methodology for  
566 computing ET<sub>0</sub> with limited data, ICID 21st European Regional Conference,  
567 Frankfurt and Slubice, 13pp.

568 Priestley, C.H.B. and Taylor, R.J., 1972. On assessment of surface heat flux and evaporation  
569 using large-scale parameters. *Monthly Weather Review*, 100: 81-92.

570 R Development Core Team, 2007. R: A Language and Environment for Statistical  
571 Computing. R Foundation for Statistical Computing, Vienna, Austria.

572 Rigollier, C., Bauer, O. and Wald, L., 2000. On the clear sky model of the ESRA - European  
573 Solar Radiation Atlas - With respect to the Heliosat method. *Solar Energy*, 68(1): 33-  
574 48.

575 Rigollier, C., Lefevre, M. and Wald, L., 2004. The method Heliosat-2 for deriving shortwave  
576 solar radiation from satellite images. *Solar Energy*, 77(2): 159-169.

577 Rana, G. and Katerji, N., 1998. A Measurement Based Sensitivity Analysis of the Penman-  
578 Monteith Actual Evapotranspiration Model for Crops of Different Height and in  
579 Contrasting Water Status. *Theoretical and Applied Climatology*, 60(1): 141-149.

580 Saltelli, A., 2002. Making best use of model evaluations to compute sensitivity indices.  
581 *Computer Physics Communications*, 145(2): 280-297.

582 Saltelli, A., Ratto, M., Tarantola, S. and Campolongo, F., 2006. Sensitivity analysis practices:  
583 Strategies for model-based inference. *Reliability Engineering & System Safety*, 91(10-  
584 11): 1109-1125.

585 Sobol', I.M., 1993. Sensitivity analysis for non-linear mathematical model. *Mathematical*  
586 *Modeling and Computational Experiment*, 1: 407-414.

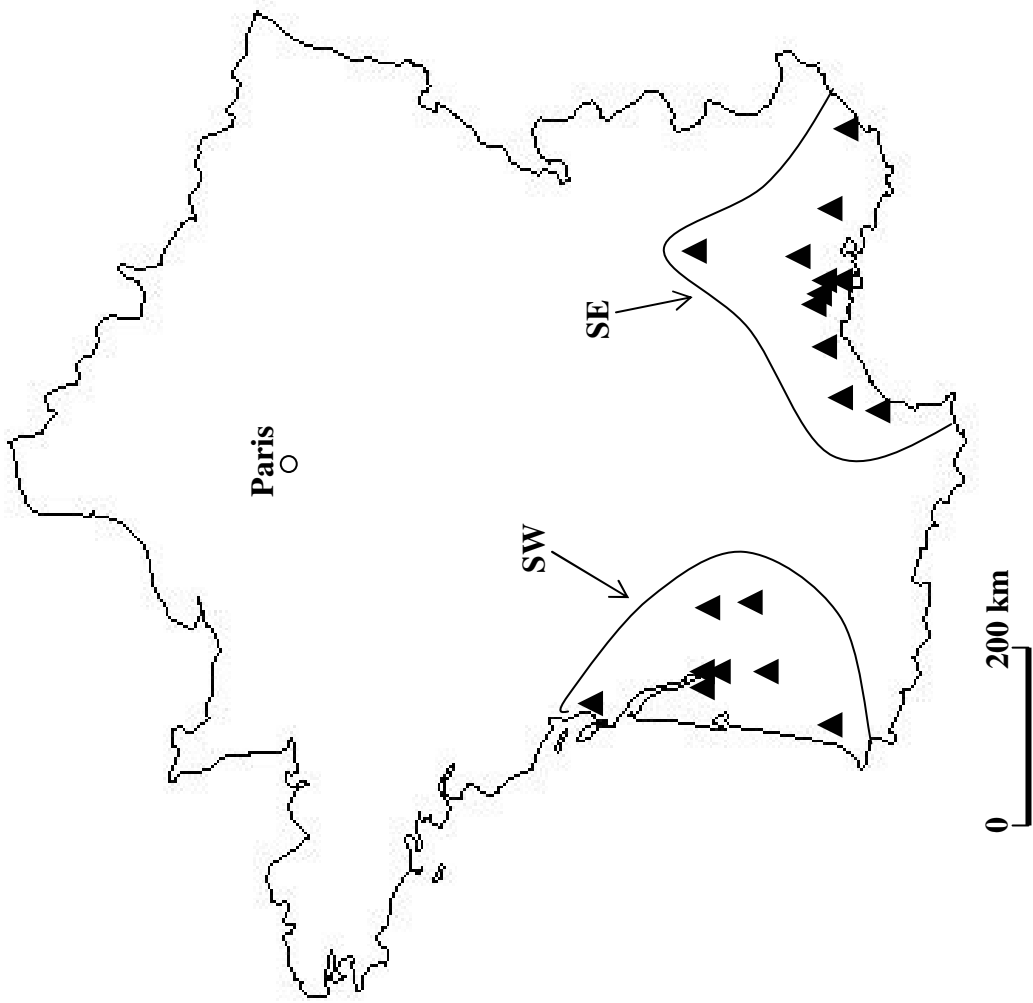
587 Struzik, P., 2001. Spatialisation of Solar Radiation - draft report on possibilities and  
588 limitations, COST action 718, 3rd Management committee and Working Group  
589 Meeting, Budapest, Hungary, pp. 12.

590 Turc, L., 1961. Evaluation des besoins en eau d'irrigation, évapotranspiration potentielle.  
591 *Annales Agronomiques*, 12(1): 13-49.

592 Xu, C.Y. and Singh, V.P., 2000. Evaluation and generalization of radiation-based methods for  
593 calculating evaporation. *Hydrological Processes*, 14: 339-349.

594 Xu, C.Y. and Singh, V.P., 2002. Cross comparison of empirical equations for calculating  
595 potential evapotranspiration with data from Switzerland. *Water Resources*  
596 *Management*, 16(3): 197-219

597 Zelenka, A., Perez, R., Seals, R. and Renne, D., 1999. Effective accuracy of satellite-derived  
598 hourly irradiances. *Theoretical and Applied Climatology*, 62(3/4): 199-207.  
599  
600 SoDa web site: <http://www.soda-is.org>  
601





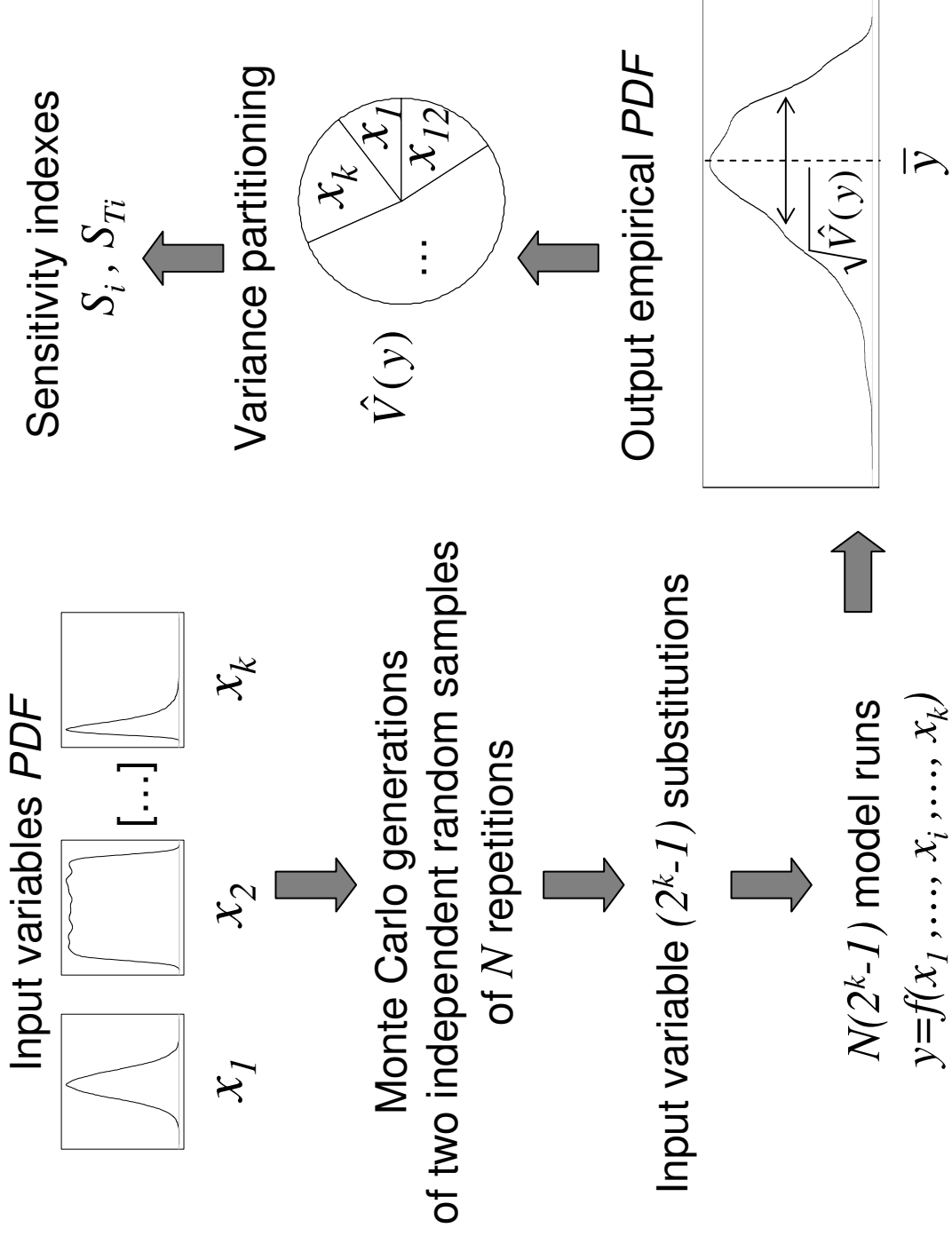
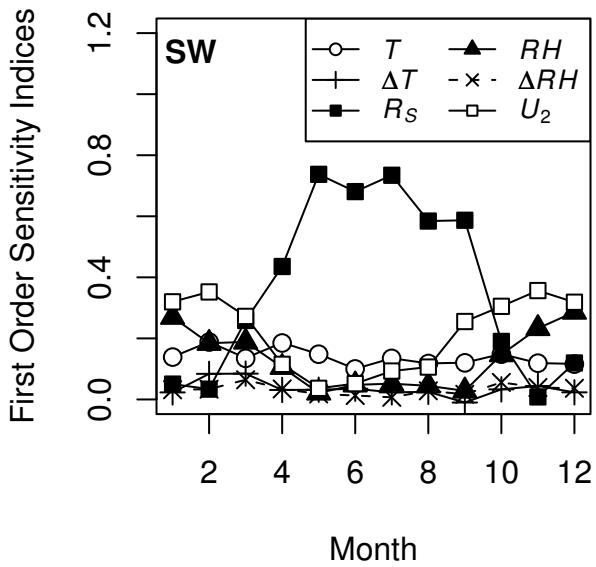
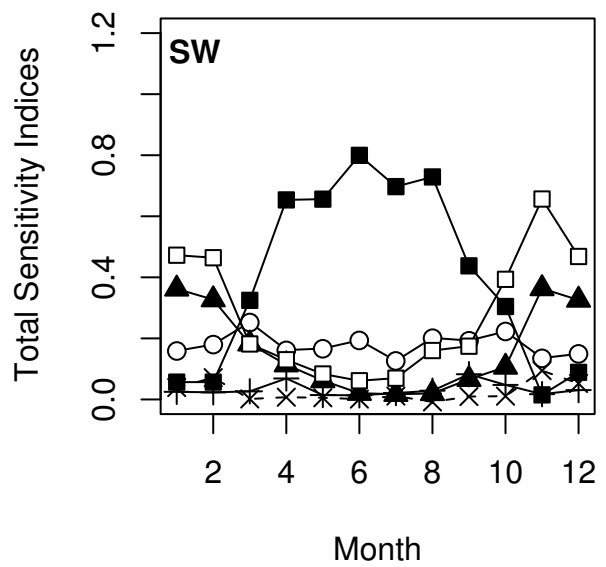


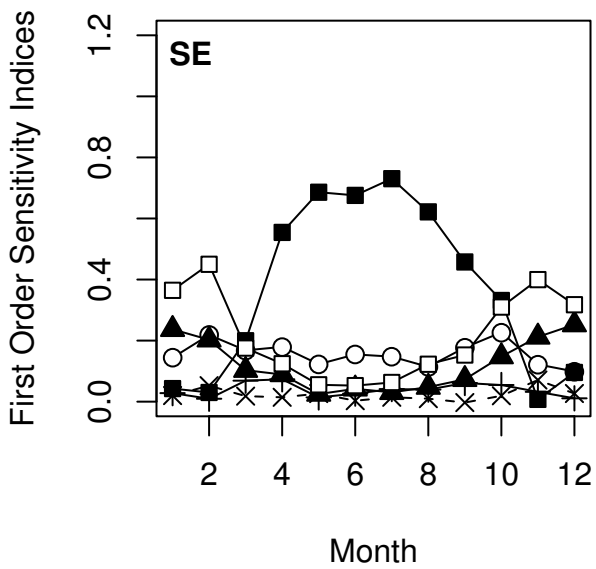
**Fig 3. SA monthly indices**



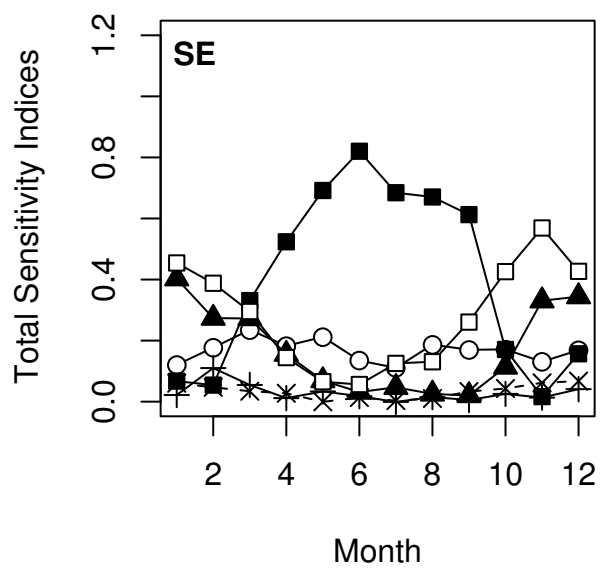
**A**



**B**



**C**



**D**

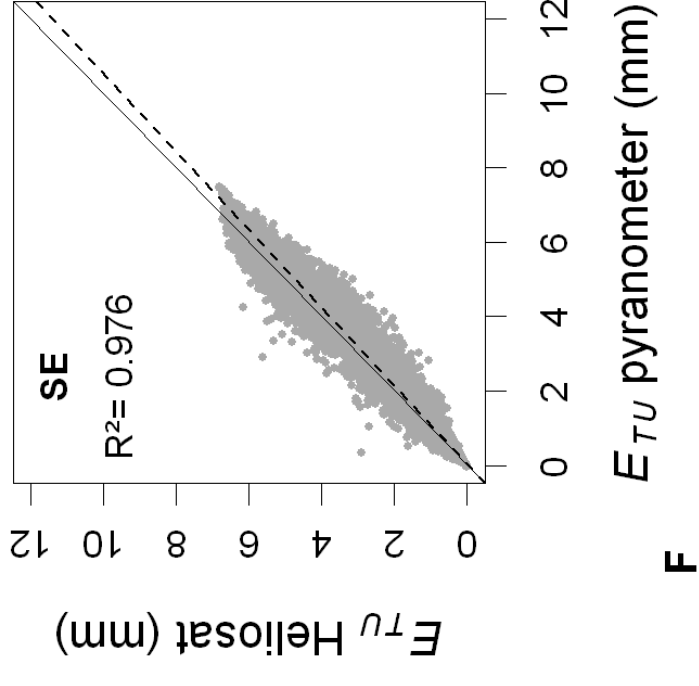
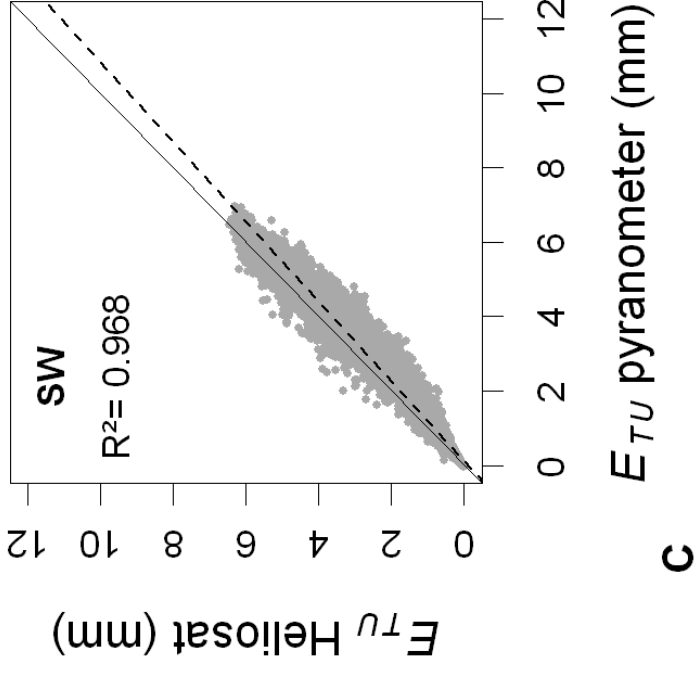
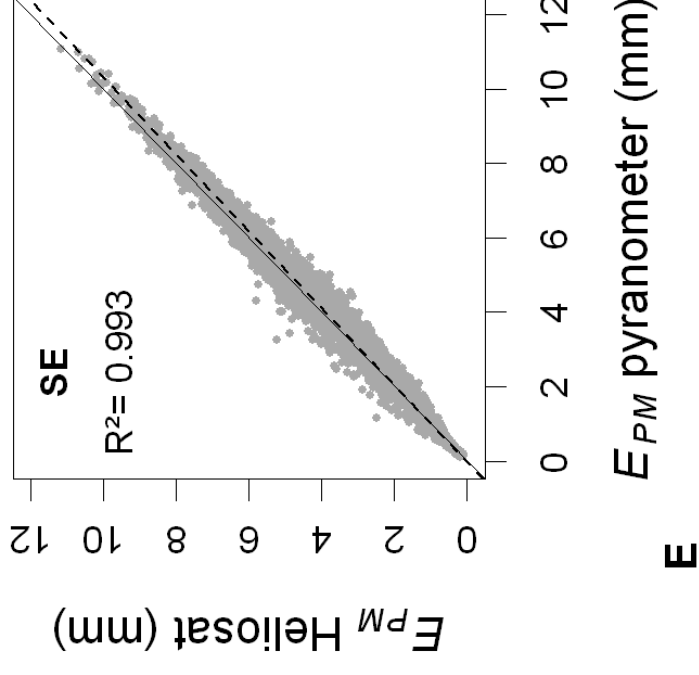
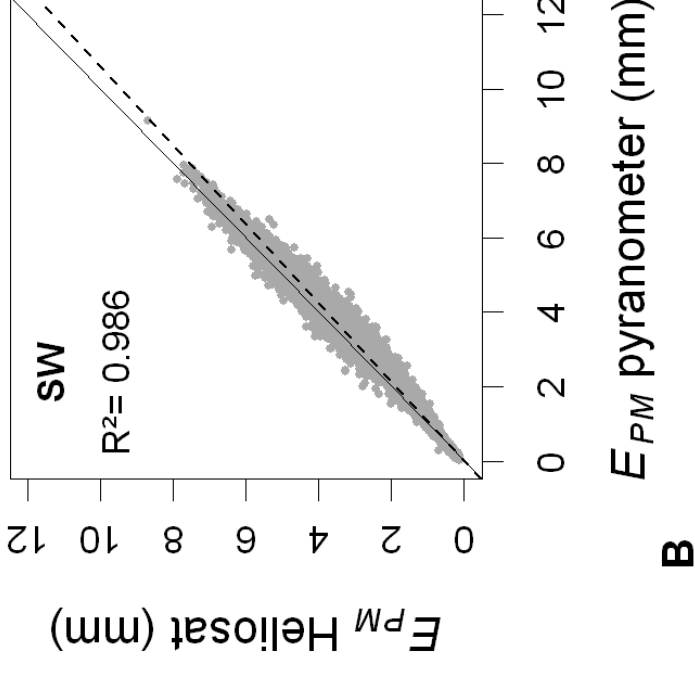
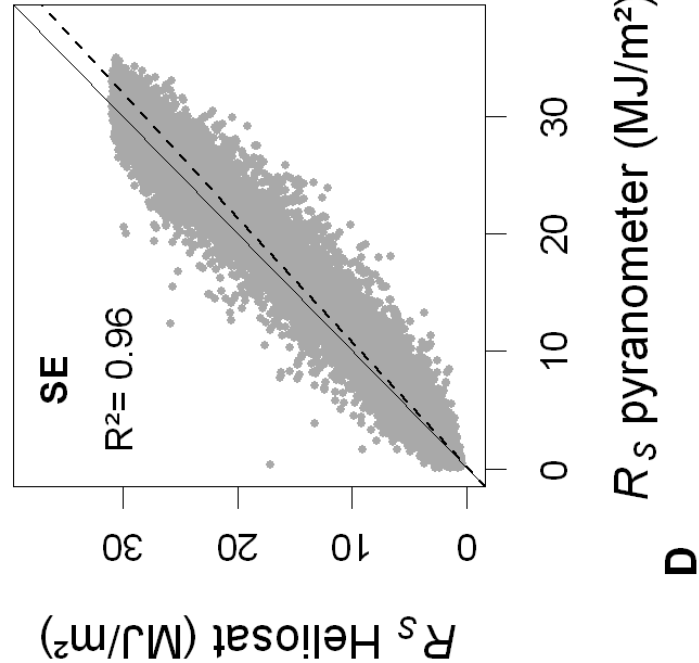
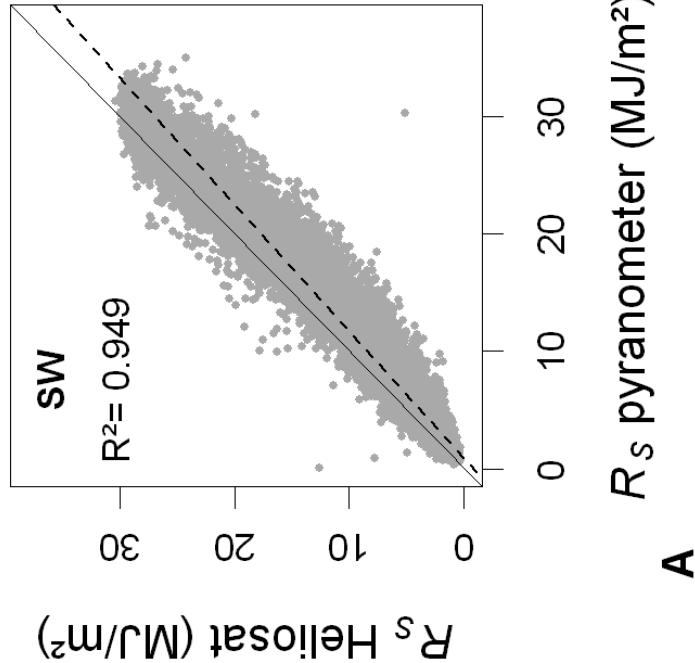


Fig 5. RMSE induced using Helioclim data by month

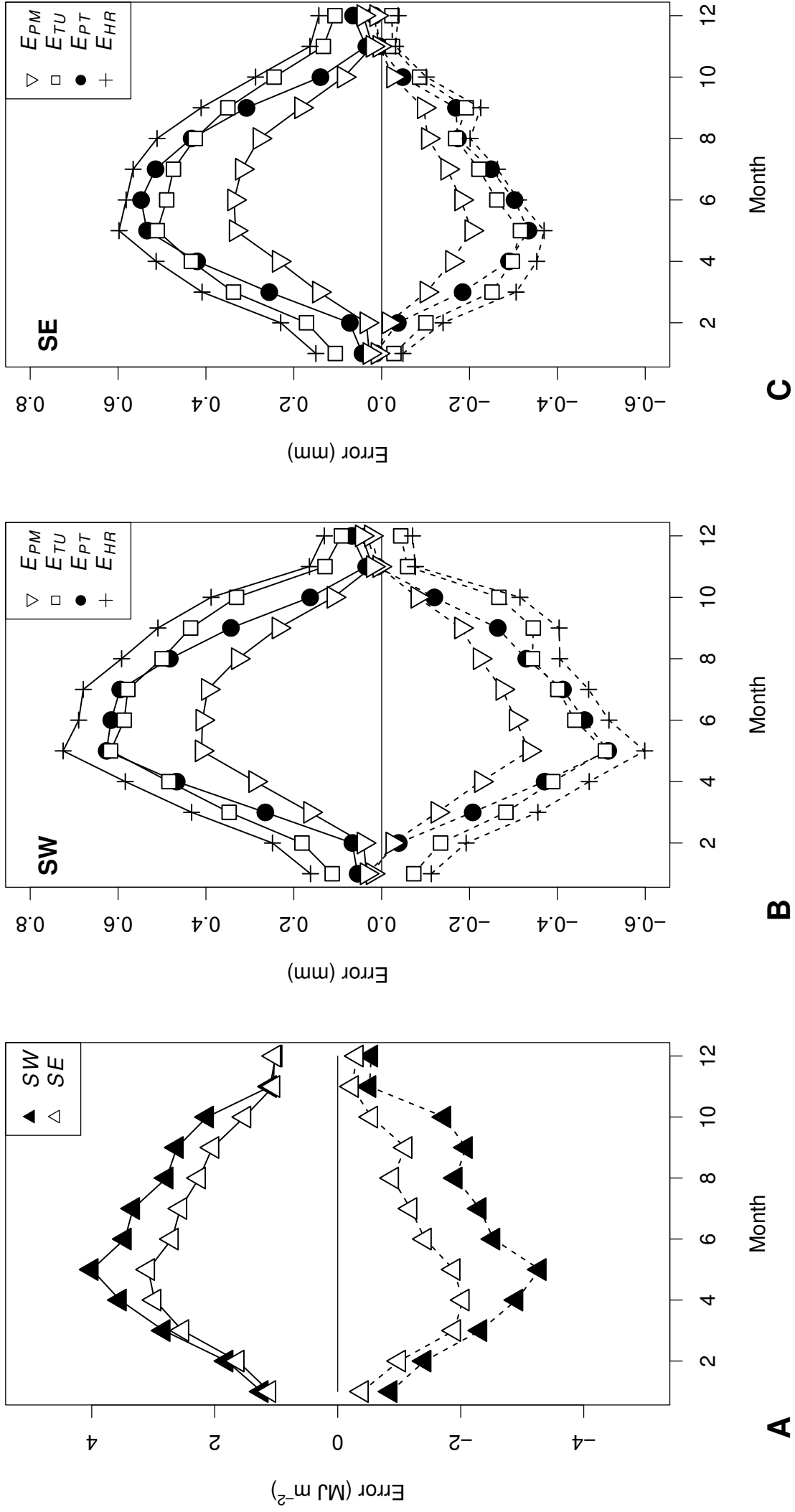
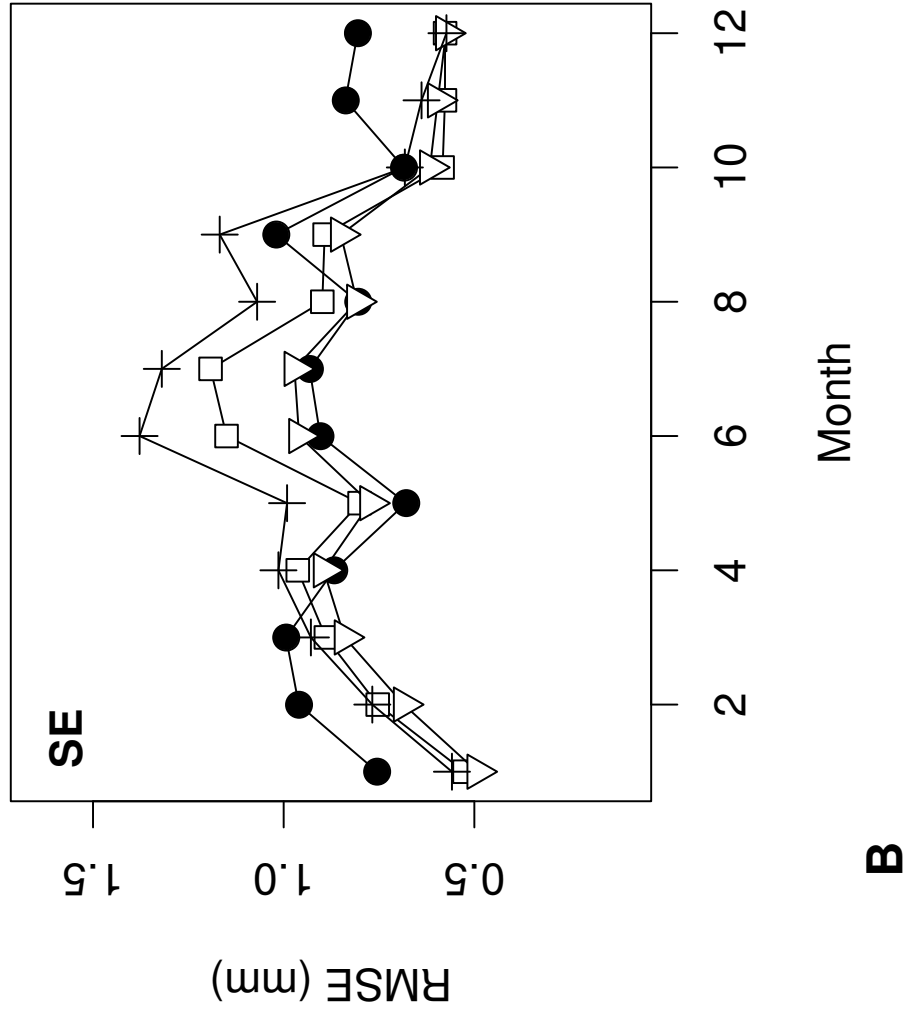
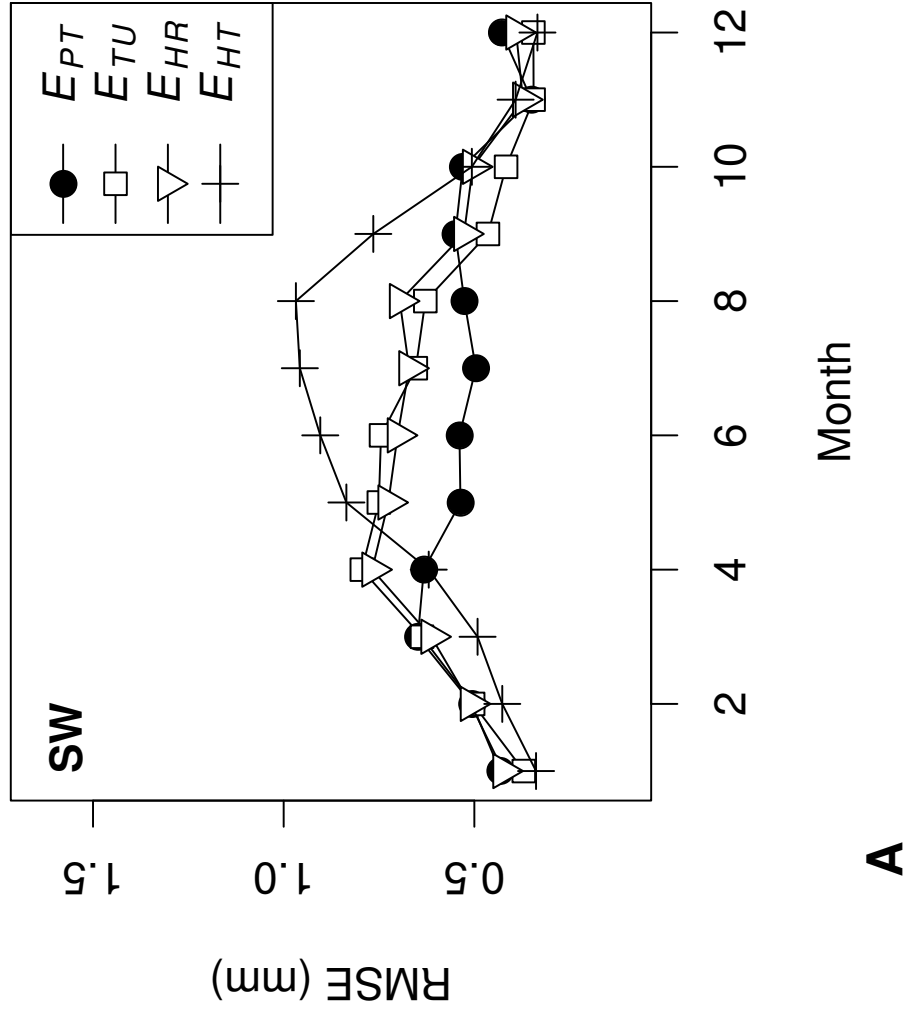


Fig 6. RMSE of empirical formulae by month



**Figure captions**

Fig. 1. Spatial distribution of the 19 meteorological stations used in the study. SW: Southwest area, SE: Southeast area.

Fig. 2. General scheme of Sobol' sensitivity analysis. *PDF* = Probability Distribution Function.  $x_i$  = the *i*th variable of the model's *k* input variables. *y* = the model output.

Fig. 3. Monthly variations of first order and total sensitivity indices of climate input variables of *PM* model, for reference evapotranspiration calculation. **A** and **B**: Southwest area (SW) ; **C** and **D**: Southeast area (SE).

Fig. 4. Scatter plots of pyranometer and HelioClim-1 data. **A, B, C**: Southwest area (SW). **D, E, F**: Southeast area (SE).  $R_s$  : daily solar irradiation ;  $E_{PM}$  :  $E_0$  daily value with Penman-Monteith (*PM*) method ;  $E_{TU}$  :  $E_0$  daily value with Turc (*TU*) method. —: (1:1) curve ; ----: linear fitting curve.

Fig. 5. Errors induced by the use of daily HelioClim-1 data for irradiation (**A**), and  $E_0$  estimates (**B**: Southwest area, **C**: Southeast area). *PM*: Penman-Monteith, *PT*: Priestley-Taylor, *TU*: Turc, *HR*: Hargreaves radiation, *HT*: Hargreaves temperature. —: RMSE ; ----: Bias.

Fig. 6. Monthly variations of RMSE resulting from the comparison of daily  $E_0$  between Penman-Monteith and estimation formulae (*PT*: Priestley-Taylor, *TU*: Turc, *HR*: Hargreaves radiation, *HT*: Hargreaves temperature). **A**: Southwest area ; **B**: Southeast area.

Table 1  
List of weather stations used in the study

# code	Site	Latitude N (°)	Longitude W (°)	Elevation (m)	Mean $E_0$ (mm d <sup>-1</sup> ) <sup>a</sup>	N <sup>b</sup>
South West						
1	BERGERAC	44.855	-0.521	33	2.34	1783
2	BOURRAN	44.334	-0.413	60	2.43	1606
3	CADAUJAC	44.753	0.554	20	2.36	1827
4	LATRESNE	44.780	0.478	63	2.54	1826
5	LUXEY	44.226	0.491	101	2.30	1818
6	SAINTE LAURENT-DE-LA-PREE	45.990	1.033	3	2.46	1827
7	SAINTE MARTIN DE HINX	43.576	1.269	64	2.29	1826
8	VILLENAVE D'ORNON	44.789	0.578	25	2.55	1827
South East						
1	AVIGNON	43.916	-4.876	24	3.27	1827
2	BELLE GARDE	43.781	-4.477	61	3.15	1762
3	FOURQUES	43.692	-4.595	3	3.41	1826
4	FREJUS	43.434	-6.717	3	3.13	1827
5	GRUISSAN	43.137	-3.121	40	3.04	1827
6	LES-SAINTE-MARIE-DE-LA-MER	43.580	-4.499	1	3.23	1827
7	MONTPELLIER	43.647	-3.874	50	2.60	1613
8	ROUJAN	43.491	-3.321	78	2.45	774
9	SAINTE-MARCEL-LES-VALENCE	44.977	-4.930	190	2.97	1827
10	SAINTE-GILLES	43.714	-4.412	72	3.15	1775
11	SALON DE PROVENCE	43.646	-5.014	68	3.27	1604

<sup>a</sup>  $E_0$  was calculated with Penman-Monteith model (*i.e.* PM).

<sup>b</sup> Number of available  $E_0$  values (days) on the period 2000-2004. Maximum is 1827. Lower N values means that data used to calculate  $E_0$  with Penman-Monteith model (*i.e.* temperature, relative humidity, wind speed or solar radiation) were unavailable on certain days.

Table 2

First order sensitivity indices of  $PM$  method to climate variables. The values between brackets correspond to the relative part of total  $E_0$  variance explained by each input variable. Figures in bold correspond to the highest sensitivity index of each month.

	Month	$T$	$\Delta T$	$R_s$	$RH$	$\Delta RH$	$U_2$
South-West	January	0.14 (17%)	0.02 (3%)	0.05 (6%)	0.27 (32%)	0.03 (4%)	<b>0.32 (38%)</b>
	April	0.19 (20%)	0.03 (3%)	<b>0.44 (48%)</b>	0.11 (12%)	0.03 (4%)	0.12 (13%)
	July	0.13 (13%)	0.02 (2%)	<b>0.73 (70%)</b>	0.05 (5%)	0.01 (1%)	0.09 (9%)
South-East	January	0.14 (17%)	0.03 (3%)	0.04 (5%)	0.24 (28%)	0.02 (2%)	<b>0.36 (44%)</b>
	April	0.18 (17%)	0.07 (7%)	<b>0.55 (54%)</b>	0.09 (9%)	0.01 (1%)	0.12 (12%)
	July	0.15 (14%)	0.04 (4%)	<b>0.73 (71%)</b>	0.03 (3%)	0.01 (1%)	0.06 (6%)



Table 3

Bias and RMSE resulting from the use of Helioclim-1 data instead of pyranometer data for daily solar irradiation and daily  $E_0$  estimates, using Penman-Monteith or radiation methods. Values between brackets are the ratio of the statistical index with the mean reference value (pyranometer solar radiation, and evapotranspiration calculated with pyranometer data).

	South-West				South-East			
	Mean	Bias	RMSE	N <sup>a</sup>	Mean	Bias	RMSE	N <sup>a</sup>
$R_S$ (MJ m <sup>-2</sup> )	13.48	-1.87 (-14%)	2.67 (20%)	14566	15.83	-1.07 (-7%)	2.16 (14%)	18997
$E_{PM}$ (mm)	2.41	-0.14 (-6%)	0.25 (11%)	14308	3.10	-0.08 (-3%)	0.21 (7%)	18448
$E_{TU}$ (mm)	2.38	-0.27 (-11%)	0.41 (17%)	14308	2.87	-0.16 (-6%)	0.35 (12%)	18448
$E_{PT}$ (mm)	2.34	-0.22 (-9%)	0.39 (17%)	14308	2.77	-0.14 (-5%)	0.34 (12%)	18448
$E_{HR}$ (mm)	2.52	-0.33 (-13%)	0.49 (19%)	14308	3.09	-0.20 (-6%)	0.41 (13%)	18448

<sup>a</sup> Number of values.

Table 4

Sources of climate variables used for reference evapotranspiration calculations in section 3.4.

<b>Method</b>	<b>Acronym</b>	<b>Temperature</b>	<b>Solar radiation</b>	<b>Relative Humidity</b>	<b>Wind speed</b>
<b>Temperature Method</b>	<i>HT</i>	Ground <sup>a</sup>			
<b>Radiation Methods</b>	<i>PT</i>	Ground	Sat <sup>b</sup>		
	<i>HR</i>	Ground	Sat		
	<i>TU</i>	Ground	Sat		
<b>Penman-Monteith Method</b>	<i>PM</i>	Ground	Ground	Ground	Ground

<sup>a</sup> Ground : climate variable measured with the weather station devices.<sup>b</sup> Sat : Helioclim-1 data (for solar radiation).

Table 5

Summary of statistical indexes of  $E_0$  estimation methods, at daily time step. Values between brackets represent the bias and the RMSE divided by  $PM$  mean values (relative bias and relative RMSE).  $R^2$  is the coefficient of determination;  $N_{SW}$  and  $N_{SE}$  are the number of observations for Southwest and Southeast area, respectively. Figures in bold correspond to the best performance in  $E_0$  estimates, according to the index considered.

	Method	Southwest (Oceanic climate)			Southeast (Mediterranean climate)		
		$R^2$	Bias (mm)	RMSE (mm)	$R^2$	Bias (mm)	RMSE (mm)
<b>January</b> ( $N_{SW}=1189$ ) ( $N_{SE}=1577$ )	<i>HT</i>	0.150	<b>0.08 (11%)</b>	<b>0.34 (49%)</b>	0.044	<b>-0.12 (-12%)</b>	0.56 (81%)
	<i>TU</i>	<b>0.205</b>	-0.15 (-22%)	0.37 (54%)	0.227	-0.23 (-23%)	0.53 (77%)
	<i>PT</i>	0.112	-0.29 (-42%)	0.43 (63%)	0.097	-0.57 (-59%)	0.76 (110%)
	<i>HR</i>	0.053	-0.16 (-23%)	0.42 (62%)	<b>0.255</b>	-0.17 (-18%)	<b>0.49 (72%)</b>
<b>April</b> ( $N_{SW}=1153$ ) ( $N_{SE}=1481$ )	<i>HT</i>	0.668	<b>0.17 (6%)</b>	<b>0.62 (22%)</b>	0.348	<b>-0.30 (-9%)</b>	1.01 (36%)
	<i>TU</i>	<b>0.830</b>	-0.66 (-23%)	0.80 (28%)	0.672	-0.66 (-19%)	0.96 (34%)
	<i>PT</i>	0.816	-0.46 (-16%)	0.63 (22%)	0.672	-0.53 (-15%)	<b>0.87 (31%)</b>
	<i>HR</i>	0.825	-0.57 (-20%)	0.77 (27%)	<b>0.678</b>	-0.51 (-15%)	0.90 (32%)
<b>July</b> ( $N_{SW}=1236$ ) ( $N_{SE}=1497$ )	<i>HT</i>	0.624	0.56 (13%)	0.96 (22%)	0.217	-0.53 (-9%)	1.32 (30%)
	<i>TU</i>	0.866	-0.42 (-10%)	0.65 (15%)	0.549	-0.77 (-13%)	1.19 (27%)
	<i>PT</i>	0.868	<b>-0.05 (-1%)</b>	<b>0.50 (11%)</b>	<b>0.576</b>	-0.30 (-5%)	<b>0.93 (21%)</b>
	<i>HR</i>	<b>0.869</b>	-0.13 (-3%)	0.67 (15%)	0.560	<b>-0.18 (-3%)</b>	0.97 (22%)
<b>Year</b> ( $N_{SW}=14308$ ) ( $N_{SE}=18448$ )	<i>HT</i>	0.894	0.32 (-13%)	0.67 (28%)	0.804	<b>-0.20 (-6%)</b>	0.96 (31%)
	<i>TU</i>	0.914	-0.30 (-12%)	0.58 (24%)	0.880	-0.40 (-13%)	0.84 (27%)
	<i>PT</i>	<b>0.938</b>	-0.29 (-12%)	<b>0.52 (22%)</b>	<b>0.890</b>	-0.47 (-15%)	0.86 (28%)
	<i>HR</i>	0.906	<b>-0.21 (-9%)</b>	0.59 (24%)	0.882	-0.21 (-7%)	<b>0.77 (25%)</b>